

# Synthesis and characterization of Fe<sub>3</sub>Co<sub>7</sub> alloy encapsulated in carbon nanoflasks

Rohit Kumar Rana,<sup>a</sup> Ishai Brukental,<sup>b</sup> Yosef Yeshurun<sup>b</sup> and Aharon Gedanken<sup>\*a</sup>

<sup>a</sup>Department of Chemistry, Bar-Ilan University, Ramat-Gan 52900, Israel.

E-mail: gedanken@mail.biu.ac.il

<sup>b</sup>Department of Physics, Bar-Ilan University, Ramat-Gan 52900, Israel

Received 19th December 2002, Accepted 4th February 2003

First published as an Advance Article on the web 14th February 2003

**A procedure for the synthesis of Fe<sub>3</sub>Co<sub>7</sub> alloy particles encapsulated in carbon nanoflasks is described, and subsequent evaluation of their structural and magnetic properties reported.**

There has been significant research and speculation about the synthesis, properties and potential applications of carbon nanotubes filled with other materials.<sup>1</sup> Recently, we reported on the synthesis of an apparently novel carbon structure encapsulating cobalt metal.<sup>2,3</sup> The flask-shaped carbon structure consists of a tubular part and a globular base that encapsulates the metal catalyst. The “carbon nanoflasks” (CNFs) were synthesized by decomposing Co(CO)<sub>3</sub>NO in the presence of Mg [covered with Mg(OH)<sub>2</sub> layers] at 900 °C in a specially arranged closed container. Investigation of the structure and composition of individual nanoflasks showed that the Mg metal plays a crucial role in the formation of CNFs.<sup>4</sup> Firstly, it partially covers the cobalt particles in such a way that the tube grows only from the exposed part. Secondly, it promotes the CO disproportionation reaction over these cobalt particles of comparatively larger sizes (50–800 nm) to generate CNFs. Using the same principle, we report herein on our successful attempt to encapsulate Fe–Co alloy particles in CNFs.

The technological importance of Fe–Co alloys arises from their soft magnetic properties and large magnetic inductions.<sup>5</sup> Some outstanding initial work on carbon-encapsulated particles of Fe<sub>x</sub>Co<sub>y</sub> alloy has been done by Majetich and co-workers.<sup>6</sup> They have clearly shown that these nanocomposite materials, synthesized by the arc-discharge process, have a protective carbon coating, which ensures that the alloy encapsulate is retained in the reduced state. Encapsulation of other ferromagnetic alloys, such as Fe–Ni, have also been reported in the literature.<sup>7</sup> As far as the confined magnetic materials are concerned, interesting properties can be exhibited, such as, for example, Barkhausen magnetization jumps seen in the case of iron nanowires encapsulated in aligned carbon nanotube bundles.<sup>8</sup>

The method used here to obtain Fe–Co encapsulated carbon nanoflasks† was the same as that for synthesizing the cobalt analogue.<sup>4</sup> Fig. 1 shows the XRD patterns of the sample before and after acid treatment. In the pattern of the as-synthesized sample, the intense peaks are due to MgO in a periclase structure. The less intense peaks can be assigned to Fe<sub>3</sub>Co<sub>7</sub> alloy particles with a bcc structure. Some very weak peaks are also observed and are assigned to graphite and cobalt. The presence of cobalt along with Fe<sub>3</sub>Co<sub>7</sub> alloy indicates that not all of the cobalt is incorporated into the alloy. However, the cobalt peaks disappear after the sample is acid treated. Moreover, after the acid treatment, the (002) graphitic peak becomes prominent with the removal of MgO particles by HCl. Along

with the graphitic peak, an appreciable amount of Fe<sub>3</sub>Co<sub>7</sub> having bcc symmetry is also detected, suggesting that these particles are well protected by the covering of graphene layers, which prevent them from reacting with the acid.

The CHN analysis of the as-synthesized sample showed a carbon content of 6.4 wt%. The amount of material recovered after the acid-treatment was 6.8 wt% and had a carbon content of 94 wt%. EDAX analysis of the as-prepared sample revealed an Fe to Co molar ratio of 1 : 3. However, the starting mixture had Fe and Co in a 1 : 1 ratio, thus indicating that all the iron was not recovered from the reaction cell. Assuming that the cell was leak free, the only possible explanation which can account for the rest of the iron is that it might have been coated onto the cell wall. It seems more probable for Fe(CO)<sub>5</sub> than Co(CO)<sub>3</sub>NO to be adsorbed onto the cell wall, as the decomposition temperature for the former (250 °C)<sup>9</sup> is higher than that of the latter precursor (55 °C),<sup>10</sup> which may facilitate the adsorption of metallic iron at the higher temperature. An attempt to increase the percentage of Fe(CO)<sub>5</sub> in the starting mixture resulted in the formation of fewer nanoflasks. This corroborates well with the above reasoning and with our earlier results, where only a few nanoflasks could be obtained using Fe(CO)<sub>5</sub>, compared with the amount obtained with Co(CO)<sub>3</sub>NO.<sup>2</sup> After acid treatment, the Fe to Co ratio becomes 3 : 7, which is in good agreement with the XRD results.

Fig. 2 shows transmission electron microscopy (TEM) images of the characteristic flask-like shapes of CNFs, with the Fe<sub>3</sub>Co<sub>7</sub> alloy encapsulated in the globular base. In the case of the as-synthesized material, only a few CNFs can be seen as they are mostly covered with the other catalytic materials. However, these impurities are not seen in the case of the acid-treated product and the nanoflasks are clearly visible, as shown in Fig. 2(b)–(e). Apart from the CNFs, other carbon nano-structures, such as tubes and fullerene-like cages, are also

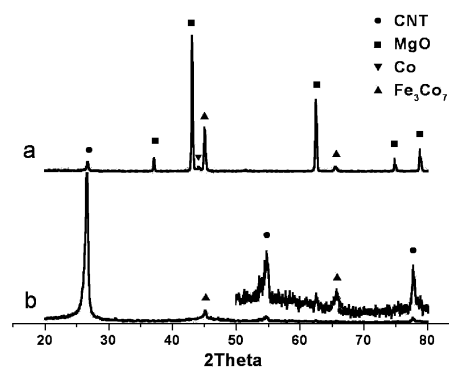
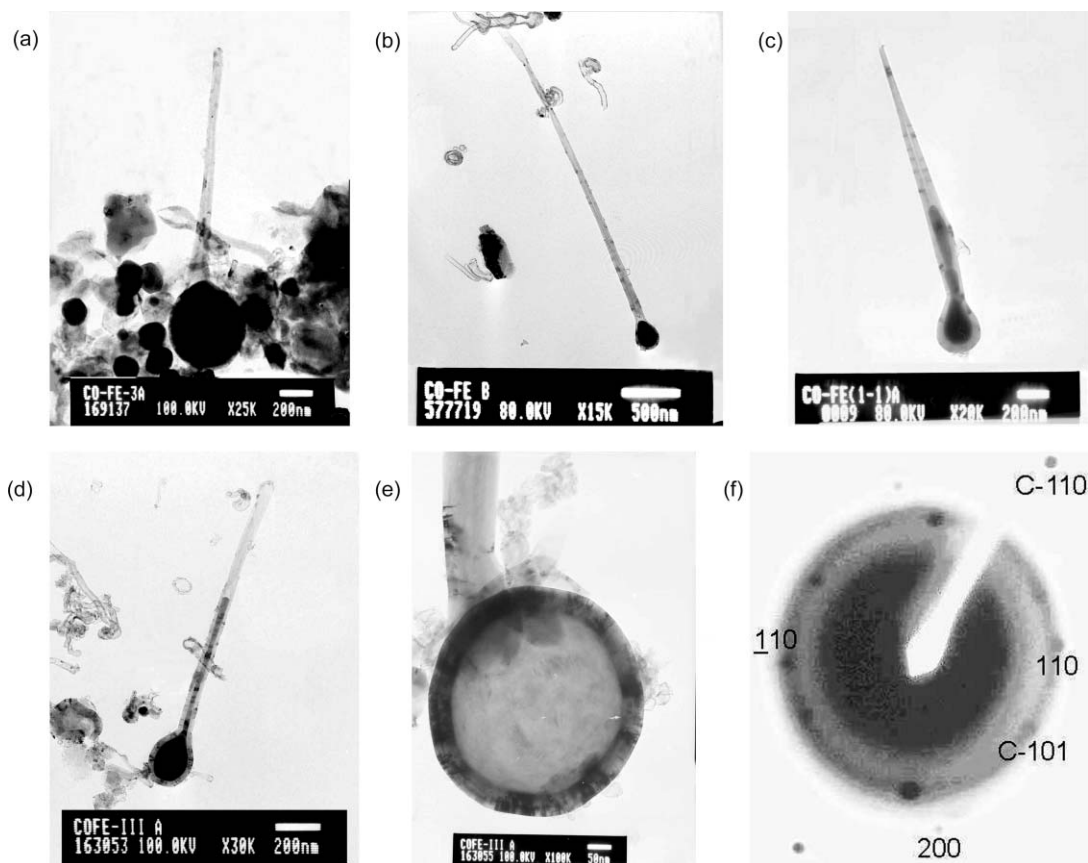


Fig. 1 XRD patterns of (a) the as-synthesized sample and (b) the acid-treated sample, with a magnified view of the portion between 50 and 80°.



**Fig. 2** Representative TEM images of (a) the as-synthesized and (b)–(e) the acid-treated sample, depicting the filled and empty CNFs. (f) The SAED pattern from the filled globular part of the CNF shown in (b) (110 and 200 spots:  $\text{Fe}_3\text{Co}_7$  alloy; C-101 and C-110 spots: carbon).

present in the sample (Fig. 2). The percentage of CNFs among all the observed structures was approximately 15%, which, as reported earlier,<sup>3</sup> can be enhanced by a magnetic separation technique. In most cases, the globular part of the CNF encapsulates an alloy particle. However, in some cases, empty nanoflasks [Fig. 2(e)] are also detected, which must be a result of the reaction of HCl with the alloy particles in uncapped CNFs. The presence of filled nanoflasks indicates a complete capping of the alloy by the graphene layers, which prevent it being leached out by HCl. In a few cases, filling of the tubular part with the alloy was also observed, as shown in Fig. 2(c) and (d). The dimensions of the globular part vary over a wide range; diameters of 100–900 nm. The outer diameters of the tubular parts vary from 30 to 100 nm and often are not uniform throughout their entire length. There is a gradual decrease in the diameter from neck to tail.

The selected area electron diffraction (SAED) pattern of the filled globular part of the CNF in Fig. 2(b) is shown in Fig. 2(f). The clear spots indicating a crystalline product can be indexed to the bcc structure of  $\text{Fe}_3\text{Co}_7$  alloy and the hexagonal structure of the surrounding graphene layers. The calculated interplanar distances are listed in Table 1, along with the known values. The brightest, innermost ring was indexed to the 002 reflection of hexagonal graphite. It gives an average

**Table 1** SAED data recorded from the globular parts of the nanoflasks

Measured $d(\pm 0.05)\text{\AA}$	Reported $d'/\text{\AA}$	Assignment ( $hkl$ )
2.05	2.04	C-101
2.06	2.01	$\text{Fe}_3\text{Co}_7$ -110
1.46	1.42	$\text{Fe}_3\text{Co}_7$ -200
1.23	1.23	C-110

<sup>a</sup>Reported  $d$  values from the JCPDS files for  $\text{Fe}_3\text{Co}_7$  and carbon (no. 48-1818 and 41-1487, respectively).

graphitic interlayer spacing of 3.4 Å, corresponding to a turbostratic structure.<sup>11</sup>

The magnetic properties of the samples were investigated at room temperature using a vibrating sample magnetometer. As can be seen in Fig. 3, at low fields range, typical ferromagnetic behavior is observed, which, above 8000 G, becomes diamagnetic with a negative magnetic susceptibility. The pure carbon nanotubes are known to exhibit a greater diamagnetic susceptibility compared with graphite.<sup>12</sup> Thus, the decrease in magnetization with increasing applied magnetic field above 8000 G is indicative of an additive effect of ferromagnetic saturation of the cobalt magnetization and a diamagnetic decrease in the magnetization of the CNFs.<sup>13</sup>

The low value of the saturation magnetization is a consequence of the small number of alloy particles present in

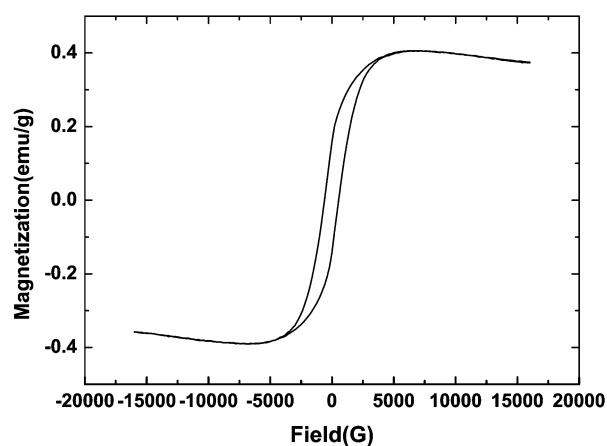


**Fig. 3** Magnetic hysteresis loop,  $M(H)$ , at RT for the acid-treated sample.

the sample (~5 wt%). The measured coercive force is 570 G, which is much higher than the values previously known for bulk alloys (which amount to a few Gauss). The  $H_c$  value is also higher than the values (200–400 G) reported for carbon-coated nanocrystalline Fe–Co alloys of ~50 nm average diameter; these particles were considered to be of a single domain structure.<sup>6,14</sup> Generally, in nanocomposite magnetic materials,  $H_c$  increases with increasing grain size when the grains are isolated and exchange decoupled. On the other hand, in the case of a multidomain structure,  $H_c$  decreases rapidly with increasing grain size because of strong exchange interactions with neighboring grains. The higher coercivity in our case thus indicates that the encapsulated Fe–Co alloys are of a large grain size with weak intergrain exchange coupling near the percolation threshold.<sup>15</sup>

In conclusion, we have successfully prepared a  $\text{Fe}_3\text{Co}_7$  alloy encapsulated in carbon nanoflasks by a direct catalytic process carried out at a lower temperature compared with the conventional high temperature arc-discharge methods. The above result evidently suggests that the  $\text{Fe}_3\text{Co}_7$  alloy particles are formed from the decomposition of a mixture  $\text{Co}(\text{CO})_3\text{NO}$  and  $\text{Fe}(\text{CO})_5$  at an elevated temperature. The close similarity between the Fe–Co- and Co-encapsulating CNFs reported previously further indicates that a similar kind of growth mechanism is involved in the formation of the nanoflasks, wherein Mg promotes the CO disproportionation reaction over these catalysts. Further work to separate the encapsulated Fe–Co particles and to study their properties is in progress.

## Notes and references

†In a typical preparation, 400 mg Mg–EtOH powder [prepared by treating fresh Mg powder (Merck) with a mixture of ethanol and water at RT for 48 h and then drying under vacuum] was inserted into a 2 ml closed cell, which was assembled from stainless steel Swagelok parts. A mixture of 350 mg each of  $\text{Co}(\text{CO})_3\text{NO}$  and  $\text{Fe}(\text{CO})_5$  (STREM) was then added to the cell under an inert atmosphere of nitrogen (glove

box). The filled cell was heated in a furnace to 900 °C at a heating rate of 20 °C min<sup>-1</sup> for 3 h. The as-synthesized black product was treated with 30% dilute HCl solution, centrifuged and then repeatedly washed with de-ionized water and ethanol to obtain the purified material.

- (a) C. N. R. Rao, B. C. Satishkumar, A. Govindaraj and M. Nath, *Chem. Phys. Chem.*, 2001, **2**, 78; (b) H. Dai, *Acc. Chem. Res.*, 2002, **35**, 1035; (c) A. Peigney, E. Flahaut, C. Laurent, F. Chastel and A. Rousset, *Chem. Phys. Lett.*, 2002, **352**, 20; (d) S. Subramoney, *Adv. Mater.*, 1998, **10**, 1157.
- S. Liu, X. Tang, Y. Mastai, I. Felner and A. Gedanken, *J. Mater. Chem.*, 2000, **10**, 2502.
- S. Liu, S. Boeshore, A. Fernandez, M. J. Sayagues, J. E. Fischer and A. Gedanken, *J. Phys. Chem. B*, 2001, **105**, 7606.
- R. K. Rana and A. Gedanken, *J. Phys. Chem. B*, 2002, **106**, 9769.
- (a) F. Pfeifer and C. Radeloff, *J. Magn. Magn. Mater.*, 1980, **19**, 190; (b) M. Rajkovic and R. A. Buckley, *Met. Sci.*, 1981, **15**(1), 21.
- (a) Z. Turgut, J. H. Scott, M.-Q. Huang, S. A. Majetich and M. E. McHenry, *J. Appl. Phys.*, 1998, **83**, 6468; (b) Z. Turgut, M.-Q. Huang, K. Gallagher, M. E. McHenry and S. A. Majetich, *J. Appl. Phys.*, 1997, **81**, 4039.
- (a) N. Grobert, M. Mayne, M. Terrones, J. Sloan, R. E. Dunin-Borkowski, R. Kamalakaran, T. Seeger, H. Terrones, M. Rühle, D. R. M. Walton, H. W. Kroto and J. L. Hutchison, *Chem. Commun.*, 2001, 471; (b) H. Q. Wu, X. W. Wei, M. W. Shao, J. S. Gu and M. Z. Qu, *J. Mater. Chem.*, 2002, **12**, 1919; (c) Y. Bando, K. Ogawa and D. Golberg, *Chem. Phys. Lett.*, 2001, **347**, 349.
- B. C. Satishkumar, A. Govindaraj, P. V. Vanitha, A. K. Raychaudhuri and C. N. R. Rao, *Chem. Phys. Lett.*, 2002, **362**, 301.
- D. Nicholls, in *Comprehensive Inorganic Chemistry*, vol. 3, ed. J. C. Bailar, Jr., H. J. Emeleus, R. Nyholm and A. F. Trotman-Dickenson, Pergamon, Oxford, 1973, p. 990.
- Catalog no. 17, Strem Chemicals, Inc., 1997–1999.
- Y. Saito and T. Yoshikawa, *Phys. Rev. B*, 1993, **48**, 1907.
- A. P. Ramirez, R. C. Haddon, O. Zhou, R. M. Fleming, J. Zhang, S. M. McClure and R. E. Smalley, *Science*, 1994, **265**, 84.
- R. K. Rana, X. N. Xu, Y. Yeshurun and A. Gedanken, *J. Phys. Chem. B*, 2002, **106**, 4079.
- Z. D. Zhang, J. G. Zhang, I. Skorvaneck, G. H. Wen, J. Kovac, F. W. Wang, J. L. Yu, Z. J. Li, X. L. Dong, S. R. Jin, W. Liu and X. X. Zhang, *J. Phys: Condens. Matter*, 2001, **13**, 1921.
- C. L. Chien, *J. Appl. Phys.*, 1991, **69**, 5257.